Jurnal Mekanikal
December 2008, No. 27, 42 - 50

SIMULATION OF NATURAL CONVECTION HEAT TRANSFER IN AN ENCLOSURE USING LATTICE BOLTZMANN METHOD

Nor Azwadi Che Sidik*, Rosdzimin, A.R.M.

Faculty of Mechanical Engineering,
Universiti Teknologi Malaysia,
81310 UTM, Skudai,
Johor

ABSTRACT

In this paper, the thermal lattice Boltzmann method (LBM), a numerical tool based on particle distribution function is used to simulate steady state thermal fluid flow problems and compared with the established CFD tools; FLUENT. At low Rayleigh number simulation, D2Q9 lattice model was coupled with the simplest D2Q4 lattice model to represent density and internal energy density distribution function respectively. While at high Rayleigh number simulation, D2Q9 lattice model was used for both density and internal energy distribution functions. Simulation of natural convection of air in a rectangular enclosure with localized heating from below and symmetrical cooling from the sides was carried out. The paper demonstrates that the lattice Boltzmann model is a promising simulation tool for the simulation of natural convection heat transfer phenomena within a wide range of Rayleigh number values.

Keywords: *Lattice Boltzmann, natural convection, internal energy distribution function*

1.0 INTRODUCTION

For more than a decade, lattice Boltzmann method (LBM) has been demonstrated to be a very effective numerical tool for a broad variety of complex fluid flow phenomena that are problematic for conventional methods [1, 2, 3]. Compared with traditional computational fluid dynamics, LBM algorithms are much easier to be implemented especially in complex geometries and multi component flows [4]. Historically, LBM was derived from lattice gas (LG) automata [5]. It utilizes particle distribution function to describe collective behaviors of fluid molecules. The macroscopic quantities such as density, velocity and temperature are then obtained through moment integrations of distribution function.

Generally, there are three types of thermal lattice Boltzmann models have been proposed; multi-speed model [6], passive scalar model [7] and double-distribution function (DDF) model [8]. Among these models, the DDF model is reported to be

* Corresponding author: E-mail: azwadi@fkm.utm.my

the most stable [9] and widely used in simulating thermal fluid flow problems [10,11]. The DDF model, used in this research, is based on the work of He et al. [8] and Luo and He [12]. This model introduces an internal energy density distribution function in order to simulate the temperature field. It has been shown that this model is simple and applicable to problems with different Prandtl numbers. More importantly, this model requires low order moment and thus provides higher numerical stability than the multi-speed and passive-scalar models. In order to verify the proposed model with different microscopic velocity, a natural convection of air in a rectangular enclosure with localized heating from below and symmetrical cooling from the sides was considered. The CFD software, FLUENT version 6.1 was used to simulate a similar problem in order to compare the proposed approach.

2.0 DOUBLE-POPULATION FUNCTION THERMAL LBM

The governing equations of the DDF thermal LBM are [8]

$$\frac{\partial f}{\partial t} + \mathbf{c}\frac{\partial f}{\partial \mathbf{x}} = \Omega(f) + F_f \tag{1}$$

$$\frac{\partial g}{\partial t} + \mathbf{c}\frac{\partial g}{\partial \mathbf{x}} = \Omega(g) \tag{2}$$

where the density distribution function $f = f(\boldsymbol{x},c,t)$ is used to simulate the density and velocity fields, and the internal energy density distribution function $g = g(\boldsymbol{x},c,t)$ is used to simulate the macroscopic temperature field. **c** in Equation (1) and Equation (2) is the microscopic velocity, Ω is the collision term and F_f is the external force. The original version of collision term was very complicated. One needs to apply the probability function in order to predict the direction of each particle distribution function after the collision process at each node. In 1954, Bhatnagar-Gross-Krook [13] proposed a simplified version of the collision term where part of the particle distribution function relaxes to the equilibrium condition after the collision. This idea was applied to the lattice Boltzmann scheme to replace the original version of collision term and is known as the lattice BGK collision model. However, the relaxation time of energy carried by the particles to its equilibrium is different from that of the momentum. Therefore two different relaxation times need to be used to characterize the momentum and energy.:

$$\Omega(f) = \frac{1}{\tau_f}\left(f^{eq} - f\right) \tag{3}$$

$$\Omega(g) = \frac{1}{\tau_g}\left(g^{eq} - g\right) \tag{4}$$

The equilibrium distribution functions are defined as

$$f^{eq} = \rho\left(\frac{1}{2\pi RT}\right)\exp\left(-\frac{\mathbf{c}^2}{2RT}\right)\left[1+\left(\frac{\mathbf{c}\cdot\mathbf{u}}{RT}\right)+\frac{(\mathbf{c}\cdot\mathbf{u})^2}{2(RT)^2}-\frac{\mathbf{u}^2}{2RT}\right] \tag{5}$$

$$g^{eq} = T\left(\frac{1}{2\pi RT}\right)\exp\left(-\frac{\mathbf{c}^2}{2RT}\right)\left[1+\left(\frac{\mathbf{c}\cdot\mathbf{u}}{RT}\right)\right] \tag{6}$$

where R is the ideal gas constant and ρ, $\boldsymbol{u}$, and T are the macroscopic density, velocity, and temperature respectively. In order to apply the LB scheme into the digital computer, the evolution equations need to be discretised in velocity space. Details of the discretization procedure can be found in [11]. As a result, the expression for the discretised equilibrium density distribution function is

$$f_i^{eq} = \rho\omega_i\left[1+3\mathbf{c}_i\cdot\mathbf{u}+4.5(\mathbf{c}\cdot\mathbf{u})^2-1.5\mathbf{u}^2\right] \tag{7}$$

and

$$g_i^{eq} = T\omega_i\left[1+3\mathbf{c}_i\cdot\mathbf{u}\right] \tag{8}$$

for internal energy density distribution function. The value of ω in Equation (7) and Equation (8) depends on the direction of the microscopic velocity, $\mathbf{c}_i$ of the particle distribution function. In this paper, nine directions of microscopic velocity model D2Q9, for density distribution and four directions, D2Q4 for internal energy distribution function are chosen. The respective lattice geometries are shown in Figure 1.

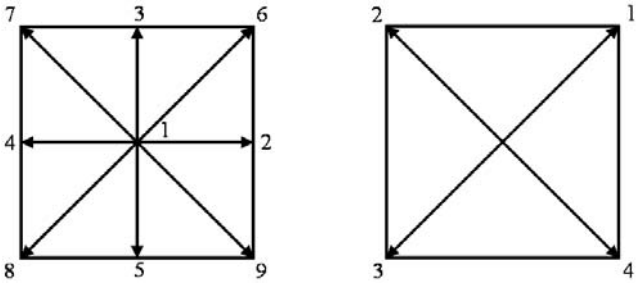

(a) (b)

Figure 1: (a) D2Q9 velocity model, $\omega_0 = 4/9$, $\omega_{1\text{-}4} = 1/9$, $\omega_{5\text{-}8} = 1/36$
(b) D2Q4 velocity model, $\omega_{1\text{-}4} = 1/4$

The macroscopic variables, such as density ρ, velocity $\boldsymbol{u}$, and temperature T can be evaluated as the moment of the distribution function

$$\rho = \int f d\mathbf{c}, \qquad \rho\mathbf{u} = \int \mathbf{c} f d\mathbf{c}, \qquad T = \int g d\mathbf{c} \tag{9}$$

By applying the Chapmann-Enskog expansion, the above equations can lead to the macroscopic continuity, momentum and energy equation. Detail derivation can be

found in [14] and [15] and will not be shown here. The viscosity υ, and thermal diffusivity χ, in these models are related to the time relaxations as follows:

$$\tau_f = 3\upsilon + 0.5, \qquad \tau_g = \chi + 0.5 \tag{10}$$

3.0 NUMERICAL SIMULATIONS

In this section, the proposed model is applied to simulate natural convection in a square cavity with localized heating from below and symmetrical cooling from the sides. Symmetrical cooling from the sides is expected to be an efficient cooling option, while partial heating at the lower surface simulates the electronic components such as chips [16]. The temperature difference between the partial bottom wall and other walls introduces a temperature gradient in a fluid, and the consequent density difference induces a fluid motion, that is, convection. Figure 2 shows a schematic diagram of the setup in the simulation. No-slip boundary conditions [5] are imposed on all the faces of the square with width, *H*. The thermal conditions applied on the walls are depicted in Figure 2. The lower wall has a centrally located heat source, *l = H/5*, which is assumed to be isothermally heated at a constant temperature, T_H.

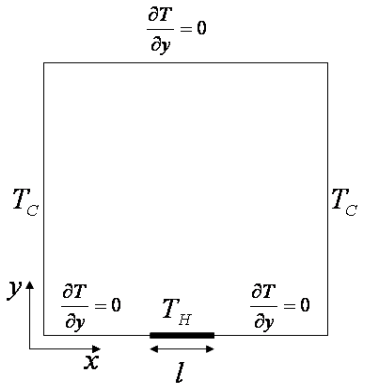

Figure 2: Geometry and boundary condition of the problem

The Boussinesq approximation is applied to the buoyancy force term as follows:

$$\mathbf{G} = \beta g(T - T_m)\mathbf{j} \tag{11}$$

where β is the thermal expansion coefficient, *g* is the acceleration due to gravity, T_m is the average temperature and **j** is the vertical direction opposite to that of gravity. Thus, the external force in Equation (1) can be written as

$$F_f = 3\mathbf{G}(\mathbf{c} - \mathbf{u}) f_i^{eq} \tag{12}$$

The dynamical similarity depends on two dimensionless parameters: the Prandtl number *Pr* and the Rayleigh number *Ra*,

$$Pr = \frac{\upsilon}{\chi},\ Ra = \frac{g\beta\Delta TH^3}{\upsilon\chi} \tag{13}$$

In all simulations, *Pr* is set to be 0.71 in order to simulate air cooling of electronic components. For low Rayleigh number simulation, *Ra* = 10^4 was selected to conduct the grid independence test. Four levels of grids namely 10, 14, 16, 18 and 20 for heated plate have been tested. Similarly for the high Rayleigh number simulation, grid 25, 30, 35 and 40 was selected and tested at *Ra* = 10^6, using the combination of D2Q9 and D2Q4 lattice model. As can be seen from Figures 3 and 4, as the grid is refined, variation in the two successive grid decreases for both cases. Grids 20 and 40 for the heated plate were chosen for all subsequent low Rayleigh and high Rayleigh number calculations by considering the relative time of computation with desirable accuracy. The following criterion is employed to check for the steady state solution:

$$\max\left|\left(\left(u^2+v^2\right)^{n+1}\right)^{\frac{1}{2}} - \left(\left(u^2+v^2\right)^{n}\right)^{\frac{1}{2}}\right| \le 10^{-7} \tag{14}$$

$$\max\left|T^{n+1} - T^{n}\right| \le 10^{-7} \tag{15}$$

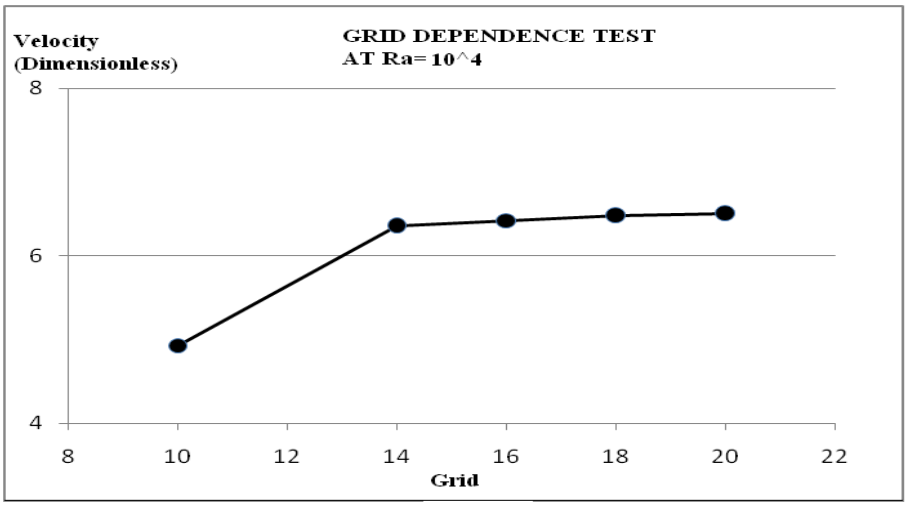

Figure 3: Grid dependence test Ra=10^4

where the calculation is carried out over the entire system. Figure 5 shows the velocity vectors for *Ra* = 10^3. They showed that the hot fluid rises above the source until it reaches the top wall, then moves outwards along the horizontal wall before moving downwards along the sidewalls under the effect of cooling. Owing to the symmetrical boundary condition, the flow reaches an asymptotic steady

state exhibiting a symmetric motion about the vertical centerline of the cavity. The flow pattern is characterized by a primary flow which consists of two counter-rotating recirculations flows delimited by a vertical thermal plume. Owing to the symmetry, the flow in the left and right halves of the enclosure is identical except for the sense of rotation.

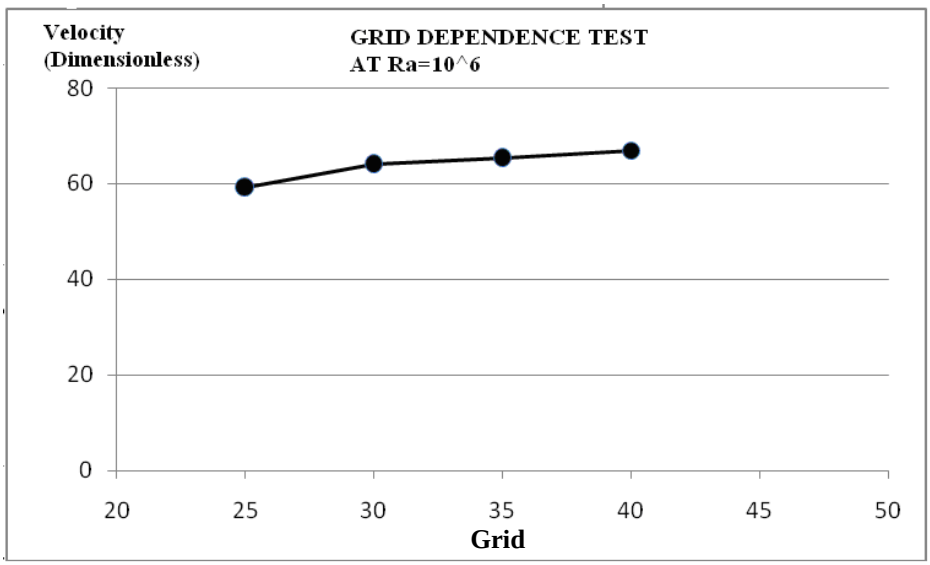

Figure 4: Grid dependence test Ra=10^6

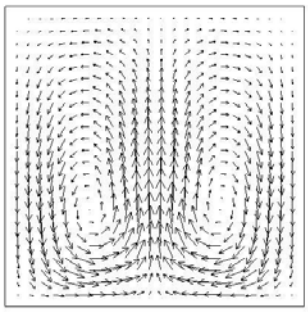

Figure 5: Velocity vector for Ra = 10^3

The main characteristics of a natural convection flow can be shown in terms of streamlines and isotherms. Figure 6 illustrates the streamline patterns for all Rayleigh numbers simulated using LBM. Owing to the symmetrical boundary condition, the flow reaches an asymptotic steady state exhibiting a symmetric motion about the vertical centerline of the cavity. The flow pattern is characterized by a primary flow which consists of two counter-rotating recirculations flows delimited by a vertical thermal plume. Owing to the symmetry, the flow in the left and right halves of the enclosure is identical except for the sense of rotation.

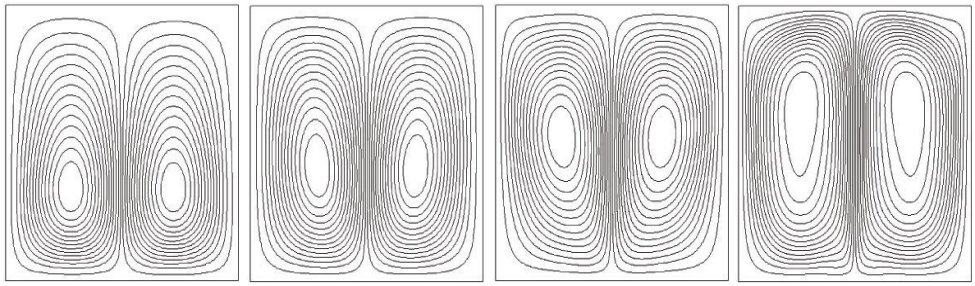

Figure 6: Streamline plots for $Ra = 10^3$, 10^4, 10^5 and 10^6 (LBM)

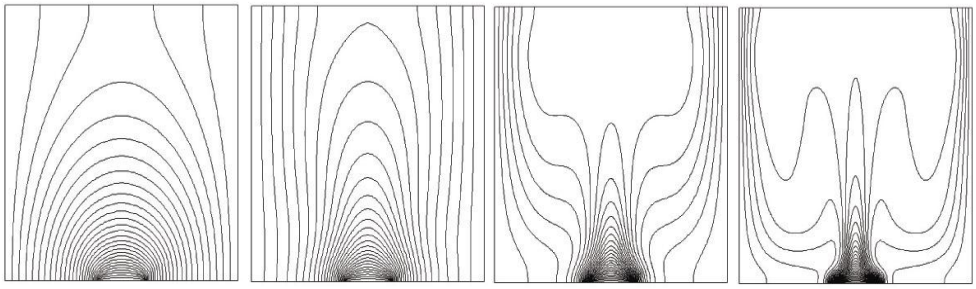

Figure 7: Isotherms for $Ra = 10^3$, 10^4, 10^5 and 10^6 (LBM)

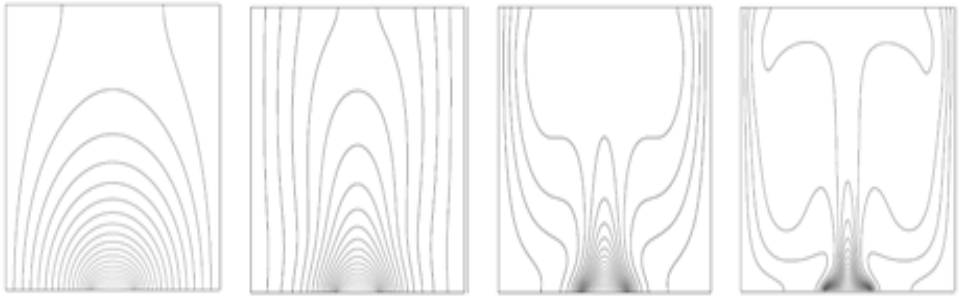

Figure 8: Isotherms for $Ra = 10^3$, 10^4, 10^5 and 10^6 (FLUENT)

Isotherms at different Rayleigh numbers simulated using LBM and FLUENT are shown in Figures 7 and 8. The results from LBM are in good agreement with the results from FLUENT. At $Ra = 10^3$, the isotherms deviate slightly from a diagonal symmetric structure indicating that most of the heat transfer is by conduction. As the Rayleigh number increases, ($Ra = 10^4$), the streamline plots show that the cores of the cells move upward and the effect of convection can be seen in isotherms due to the distortion of the isotherms. At $Ra = 10^5$, the formation of thermal boundary layer can be observed due to increased recirculation intensity. At $Ra = 10^6$, the thermal boundary layer gets thinner and the vortices grow as a result of higher fluid velocities which contributes to an increase in the overall heat

transfer. It can be seen from these figures that as the Rayleigh number increases, the intensity of recirculation increases and the cores move up to the top wall. Figure 9 show the comparisons of the results between LBM and FLUENT for the temperature profile at the mid-height of the cavity at all Rayleigh numbers. At low Rayleigh numbers, (10^3 and 10^4), the temperature profiles are typical of shear layers developing along the sidewalls. These layers are rather thick because of the low value of the considered Rayleigh number. As the Rayleigh number increases, $Ra = 10^5$, large gradients are clearly visible in the profile of temperature plotted above the heat source. At $Ra = 10^6$, these boundary layers becoming thinner due to high intensity of recirculation and heat transfer from the heat source.

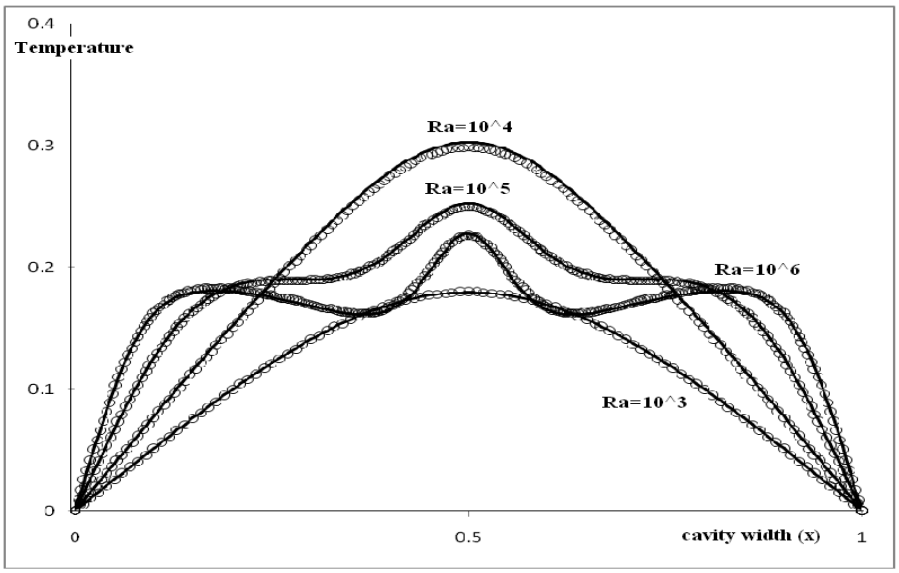

Figure 9: Temperature profiles at the mid-height of cavity for all values of Rayleigh numbers (o) LBM and (–) FLUENT

4.0 CONCLUSIONS

In this paper, the natural convection heat transfer in a square cavity with localized heating from below and symmetrical cooling from the sides has been studied using double-distribution function thermal LBM with different microscopic velocity. Our study showed that the flow pattern and heat transfer mechanism are significantly affected by the value of Rayleigh number. The demonstrated results are also in excellent agreement with those obtained from FLUENT. This indicates that the LBM approach is a promising procedure to study flow and heat transfer in a differentially heated cavity.

ACKNOWLEDGEMENTS

The authors wish to thank Universiti Teknologi Malaysia and the Malaysian Government for supporting this research activity.

REFERENCES

1. Bernsdorf, J., Brenner, G. and Durst, F., 2000. Numerical analysis of the pressure drop in porous media flow eith lattice Boltzmann (BGK) automata, *Comp. Phys. Comm*., 129, 247-255.
2. Chen, S., Martinez, D. and Mattaeus, W.H., 1994. Lattice Boltzmann magnetohydrodynamics, *Phys. of Plasmas*, 1 1850-1860.
3. Azwadi, C.S. and Tanahashi, T., 2006. Simplified Thermal Lattice Boltzmann Model in Incompressible Limit, *Proc. Asean Cong. Fluid Mech*., 11, 275-280.
4. Martys, N.S. and Chen, H., 1996. Simulation of multicomponent fluids in complex three dimensional geometries by the lattice Boltzmann method, *Phys. Rev. A*, 53, 743-750.
5. Frish, U., Hasslacher, B. and Pomeau, Y., 1986. Lattice Gas Automata for the Navier-Stokes equation, *Phys. Rev. Lett*., 56, 1505-1509.
6. McNamara, G. and Alder, B., 1993. Analysis of the lattice Boltzmann treatment of hydrodynamic, *Phys. A*, 194, 218-228.
7. Shan, X., 1997. Simulation of Rayleigh Bernard convection using a Lattice Boltzmann method, *Phys. Rev. E*, 55, 2780-2788.
8. He, X., Chen, S. and Doolen, G.D., 1998. A novel thermal model for the lattice Boltzmann method in incompressible limit, *J. Comp. Phys*., 146, 282-300.
9. Peng, Y., Shu, C. and Chew, Y.T., 2003. Simplified thermal lattice Boltzmann model for incompressible thermal flow, *Phys. Rev. E*, 68, (2003) 020671/1-020671/8.
10. Azwadi, C.S. and Takahiko, T., 2006. Simplified Thermal Lattice Boltzmann in Incompressible Limit, *Intl. J. Mod. Phys. B*, 20, 2437-2449.
11. Onishi, J., Chen, Y. and Ohashi, H., 2001. Lattice Boltzmann Simulation of natural convection in a square cavity, *JSME Intl. J. Ser. B*, 44, 53-62.
12. Luo, L.S. and He, X., 1997. A priori derivation of the lattice Boltzmann equation, *Phys. Rev. E*, 55, R6333-R6336.
13. Bhatnagar, P.L., Gross, E.P. and Krook, M., 1954. A model for collision process in gasses 1, small amplitude process in charged and neutral one component system, *Phys. Rev.*, 94, 511-525.
14. Azwadi, C.S. and Takahiko, T., 2007. Three dimensional Thermal lattice Boltzmann simulation of natural convection in a cubic cavity, *Intl. J. Mod. Phys. B*, 21, 87-96.
15. Luo, L.S. and He, X., 1997. Lattice Boltzmann model for the incompressible Navier Stokes equation, *J. Stat. Phys.*, 88, 927-944.
16. Aydin, O. and Yang, W.J., 2000. Mixed convection in cavities with a locally heated lower wall and moving sidewalls, *Num. Heat. Trans.*, 37, 695-710.